Energy 165 (2018) 925–938

Contents lists available at ScienceDirect

Energy

journal homepage: www.elsevier.com/locate/energy

Theoretical models for wall solar chimney under cooling and heating modes considering room configuration

Long Shi

Civil and Infrastructure Engineering Discipline, School of Engineering, RMIT University, Melbourne, VIC 3000, Australia

ARTICLE INFO

Article history:
Received 29 May 2018
Received in revised form
25 August 2018
Accepted 6 October 2018
Available online 8 October 2018

Keywords:
Renewable energy
Solar chimney
Trombe wall
Natural ventilation
Thermal buoyancy
Theoretical model

ABSTRACT

Under the fact that previous studies have usually ignored the influences of room configuration, wall solar chimney under both cooling and heating modes were analysed theoretically to fill the research gap. Solar chimney performance is dependent on the airflow rate and its temperature, where theoretical models were developed in this study to predict the performance of four typical types, including fresh-air cooling, fresh-air heating through chimney cavity and room, and sealed heating (without any fresh-air supply). It is known that the room configuration shows considerable influences on solar chimney performance, where a coefficient is proposed to address this. Different from the cooling mode, airflow rate under heating mode was found not only dependent on cavity height, but also the opening height of the room. To heat a typical room, fresh-air heating through the cavity shows the highest airflow rate but with the lowest temperature, which can be applied to regularly occupied building under cool weather conditions. Fresh-air heating through the room shows an opposite way, which is suitable for regularly occupied buildings under cold weather conditions. The performance of sealed heating is between these two, which can be used for non-regularly occupied buildings as there is no fresh air supply.

1. Introduction

Energy demand is continuously increasing with the rapid rise of both population and new technologies [1]. For example, fossil fuels account for about 85% (27% coal, 35% oil, and 23% natural gas) of the total energy consumption and 68% of total electricity generation worldwide [2]. To reduce the usage of fossil fuels, one of the best ways is to reduce their usages in buildings. This is because buildings are responsible for over 40% energy usage in the whole world, mainly for heating, cooling, providing electricity and air conditioning (HVAC) system [3,4]. Furthermore, renewable energy is environmental friendly with much less greenhouse gas emission [5]. Therefore, many renewable energy systems have been utilized in buildings [6], such as solar-based, ground source-based energy systems, and day-lighting system.

Solar chimney is basically a solar air heater, which is vertically or horizontally embedded as a part of wall or roof [7]. Chimney cavity normally consists of a glazing wall for solar penetration and an absorption wall for heat absorption, as shown in Fig. 1. The air in the chimney cavity is heated under the penetration of solar radiation through the glazing wall and they rise under the thermal buoyancy to enhance the natural ventilation of buildings. Solar chimney is used to promote natural ventilation by taking away indoor heat (cooling mode) or bringing in hot air (heating mode), resulting in the reduction of traditional energy use and the relevant greenhouse gas emission [8–10]. As the heated air always rises under the thermal buoyancy, flowing out or into the room can achieve cooling or heating purposes, respectively. As seen in Fig. 1, the switch between cooling and heating modes can be realized by those dampers.

Solar chimney as a reliable renewable energy system has been utilized in buildings based on solar radiation. It is different from solar photovoltaic, which cannot produce electricity directly. The energy saving is realized through promoting natural ventilation and then save the electricity on HVAC systems of a building. The reduction of HVAC energy consumption is critical as it is estimated that, for example in the USA, HVAC systems take about 50% of building energy consumption and 20% of total consumption [11,12]. The performance of a solar chimney can be reflected by the airflow rate and its temperature. Under cooling mode, as shown in Fig. 1(a), a bigger airflow rate through the chimney cavity represent taking more heat out of the building. Under heating mode shown in Fig. 1(b), a combination of airflow rate and its temperature is then

E-mail addresses: shilong@mail.ustc.edu.cn, long.shi@rmit.edu.au.

https://doi.org/10.1016/j.energy.2018.10.037
0360-5442/

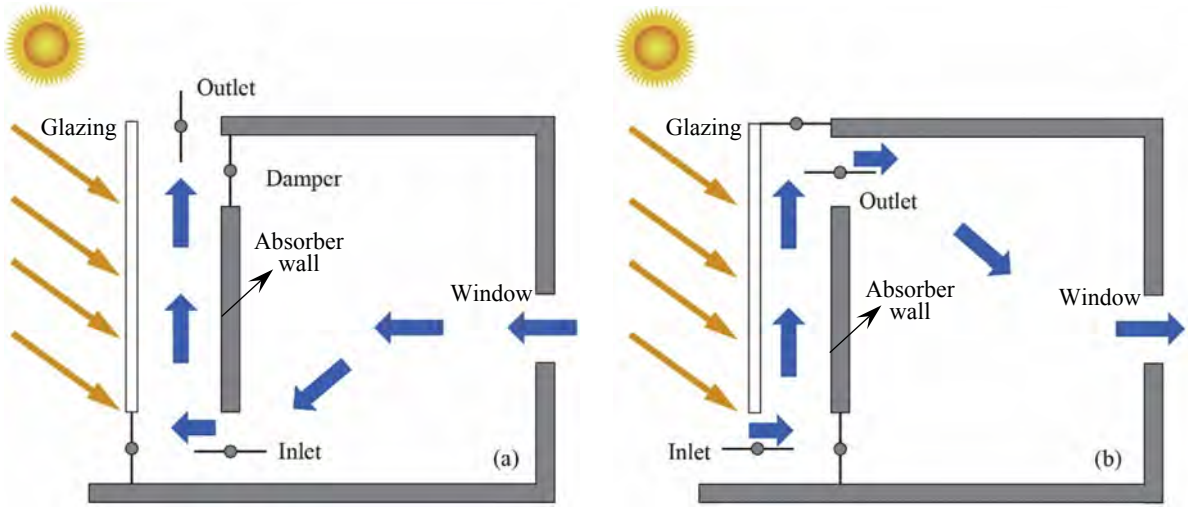

Fig. 1. Typical wall solar chimney under: (a) cooling mode; and (b) heating mode.

significant to determine the performance of a solar chimney.

Previous studies have largely focused on the cooling mode of solar chimney where the related investigations on its heating mode are limited. The heating potential of solar chimney was investigated by Lee and Strand [13] under the influences of chimney height, solar absorptance and solar transmittance of the glazing wall based on their in-house module which was developed and implemented in EnergyPlus. Ong [14,15] developed a mathematical model to predict the solar chimney performance under various ambient and geometrical conditions based on thermal resistance network. Zhai et al. [16,17] also investigated experimentally and theoretically the influences of several important factors such as inclination angle, channel gap and collector type. According to our literature review on solar chimney [18], it is known that although solar chimney has been frequently investigated, previous focuses are almost on its cooling mode, leaving very few studies on the heating mode. This may be because of the usually adopted simplified model that ignore the influences from the room configurations. Previous studies [19–21] are much focusing on experimental or numerical investigations based on solo chimney cavity. Under this simplified structure, the airflow rate can be considered the same under both cooling and heating modes. It is still unknown if this assumption is viable during the practical applications of solar chimney.

Although the importance of room configuration on solar chimney performance is clearly understood, very few studies have explored this aspect even its effect may be overwhelming while the efforts have been much on the optimization design of solo solar chimney itself. According to our recent review [18], the frequently investigated influencing factors are mainly for solar chimney independently, including configuration (e.g. height [22,23], cavity gap [24], inlet and outlet areas [25,26], and height/gap ratio [27,28]), installation conditions (e.g. inclination angle (for roof solar chimney) [22,29], opening [25] and solar collector [30]), material usages (e.g. glazing type [31], solar absorber [19,32] and thermal insulation [30]), and environment (e.g. climate [33,34], solar radiation [35,36] and external wind [37,38]).

However, those previously developed theoretical models may not be applicable when it needs to consider the influences from the room configuration under the practical applications. This results in a critical gap for the relevant designs and implementations. Furthermore, those theoretical models for solar chimney under cooling mode have been well developed [39–42]. However, it is still not known whether these models are still applicable to the heating mode. Comparing to the numerical approach, theoretical models more favor the practical implementations which can provide a fast and convenient way for the optimization design of solar chimney. Although the numerical tools can provide more detailed information about the airflow inside the chimney cavity and room, the related calculation time is much longer and the results are lacking generality.

Solar chimney under cooling mode has been largely investigated previously, but the relevant studies under heating mode is still a challenge. Firstly, different from the cooling mode, the room under heating mode is no longer a mixed ventilation, which can be considered as a two-layer problem [43,44]. The upper layer of the room is the hot air from the chimney cavity, which are gathered at the ceiling under thermal buoyancy, while the lower layer is still fresh air. Secondly, solar chimney under heating mode is complicated with many types, as seen in Figs. 3–5. It is still not clear about the airflow rate and the temperature with these typical types. It is of significance to identify the applicability of these types of solar chimney under heating mode.

Therefore, in this study, four typical types of solar chimney under both cooling and heating modes were investigated theoretically, including fresh-air cooling, fresh-air heating through the chimney cavity, fresh-air heating through the room, and sealed heating. Validation, comparisons and related implementations were also made to address their applicability. The research outcomes provide a theoretical and technical basis for the related optimization designs and implementations of solar chimney under both cooling and heating modes. Section 2 will focus on the development of theoretical models for these four solar chimney types. Section 3 presents the validation of theoretical models based on experimental data. Section 4 includes the comparison and implementations of these theoretical models, where the advantages and disadvantages of these four types of solar chimney are discussed.

2. Mathematical models

As shown in Figs. 2–5, four typical types of solar chimney can be known under cooling and heating modes, including fresh-air cooling, fresh-air heating through the chimney cavity, fresh-air heating through the room, and sealed heating. In the following section, these four types of solar chimney will be analysed one by one theoretically to predict the airflow rate and temperature

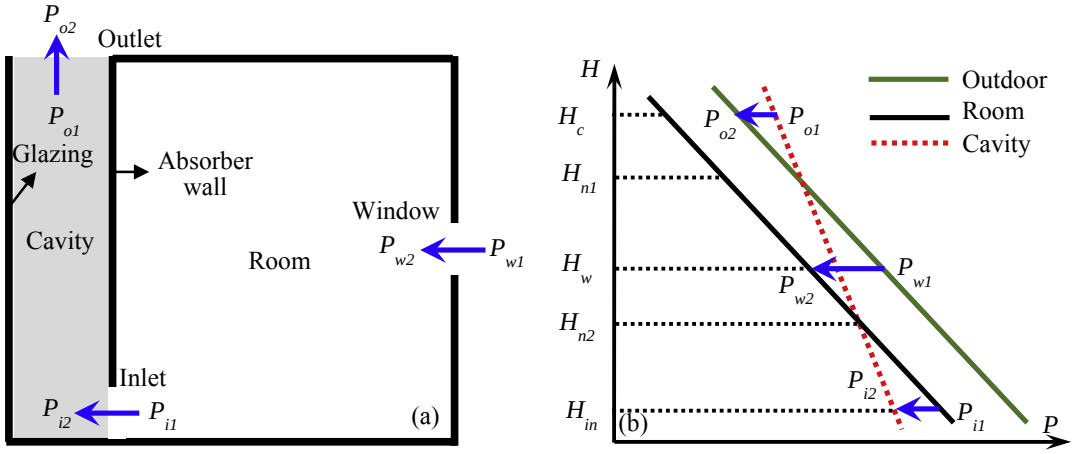

Fig. 2. Solar chimney under fresh-air cooling (a); and pressure distributions in outdoor, room and cavity (b). H_{n1} and H_{n2} are the heights of neutral planes in the room and chimney cavity, respectively.

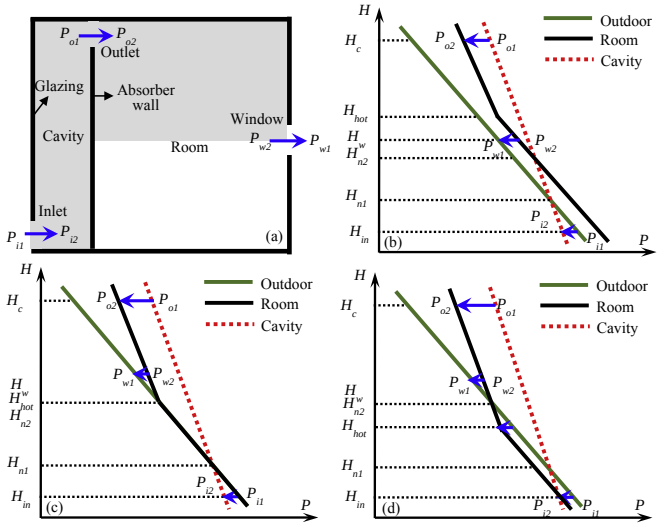

Fig. 3. Solar chimney under fresh-air heating through cavity (a) and pressure distributions under (b) unsteady scenario; (c) steady scenario; and (d) unlikely scenario.

through the chimney cavity considering the room configuration. After that, the influences of the room configuration on solar chimney performance are addressed theoretically as well.

2.1. Fresh-air cooling

Fig. 2(a) shows the solar chimney under fresh-air cooling. The left side is the chimney cavity and the right-side is the connected room. The chimney cavity is constructed by a glazing wall and an absorber wall. The glazing wall is allowing solar radiation penetration to the chimney cavity for the heating of the internal air, while the absorber wall is to absorb the solar radiation to enhance the process. The room is connected to the outdoor environment through an opening, which can be in a form of window or door. When there is solar radiation on the glazing wall, the air inside the chimney cavity rise under the effect of thermal buoyancy. After exhausting the air to the outdoor, the pressure inside the chimney cavity then drops, which results in the entry of air from the room.

Theoretical models have been developed regarding the performance of solo solar chimney, which means the solar chimney is directly connecting the ambient without connecting a room/chamber. Andersen [41,45] developed a theoretical model to predict the volumetric flow rate through a chamber with two openings under thermal buoyancy. Those previous models before Andersen were much based on the temperature gradient between the internal cavity and the ambient, while the air temperature inside the cavity cannot be obtained unless undertaking the experiment. So their practical applications are limited. Based on my understanding through the literature review, Andersen's model is the first comprehensive theoretical model for wall solar chimney with easy-to-obtained inputs such as total heat input.

Regarding the consideration of room configuration, a point needed to be mentioned that Spencer et al. [26,46] have developed a theoretical model for the natural ventilation prediction under cooling mode. In this study, the developed model under cooling model is a little different, which is simplified with the following assumptions: (a) the air inside the room (upper or lower part of room under heating mode) and chimney cavity are well mixed; (b)

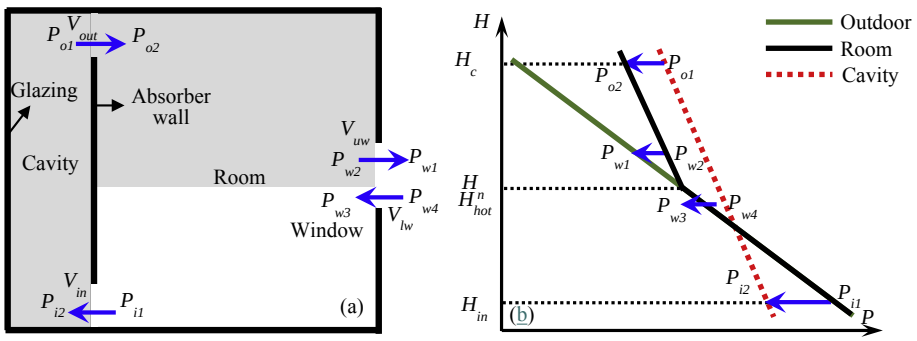

Fig. 4. Solar chimney under fresh-air heating through room (a); and (b) the pressure distributions.

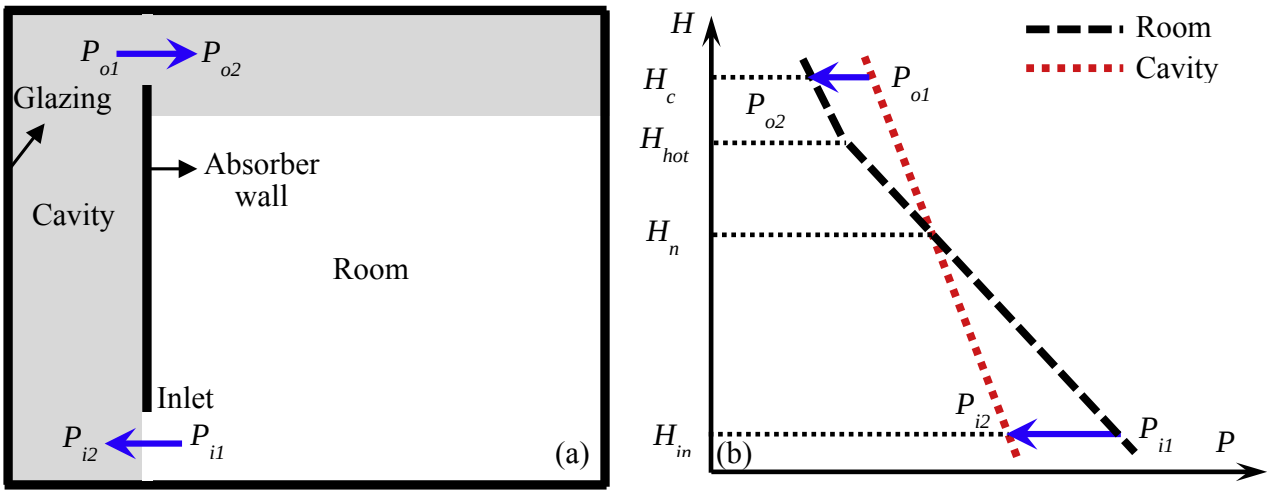

Fig. 5. Solar chimney under sealed heating (a) and the pressure distribution (b) inside chimney cavity and room.

the discharge coefficients for all the orifices are considered the same; (c) the friction losses occur in the chimney cavity are ignored due to the complexity of the problem; (d) the external wind in the outdoor environment is neglected, suggested by Afonso and Oliveira [47] and Tan and Wong [37]; and (e) This study much focuses on predicting solar chimney performance under steady status, where there is a balance of heat transfer between the walls and airflow. In order to provide the direct analytical solutions of the theoretical models, the related heat transfer between the walls and airflow inside the room were ignored. The above assumptions also apply to the heating model of solar chimney in this study.

The pressure distributions inside the ambient environment, room and chimney cavity can be seen in Fig. 2. As the air inside the room and chimney cavity are considered well mixed and uniform, hydrostatic pressure is then considered linear to the height with a changing rate of ρg. A pair of parallel lines can be used to present the hydrostatic pressure outside and in the room. The pressure distributions in outdoor environment, room and chimney cavity can be seen in Fig. 2(b), which can be given by,

$$\Delta P = \rho g \Delta H \tag{1}$$

where ΔP is the pressure difference, Pa; ρ is the density of air, kg/m^3; g is the acceleration of gravity, m/s^2; and ΔH is the difference of vertical heights, m.

As the heating power is much larger in the cavity, the slope of the pressure curve in the cavity is obviously higher than the others based on Eq. (1). It is known that the heights of neutral pressure planes are different in the cavity and the room, while the neutral plane for the cavity (H_{n1}) is higher than that of the room (H_{n2}) under the conditions. This is different to Lin and Linden's study [44] with two chambers that there is an extra opening located on the ceiling which allows the airflow along the ceiling, resulting in the same height of neutral pressure planes in both chambers.

The air through orifices, including window, air inlet and outlet, are driven by the pressure gradient, where a relationship can be obtained:

$$\Delta P_j = \frac{1}{2}\rho_j U_j^2 \tag{2}$$

where U is the air velocity through the orifice, m/s; and j is the orifice number.

For the contracted air flow through the orifice, the volumetric flow rate is less than the theoretical calculation, while the reduction rate is described by coefficient of discharge (C_d). All the orifices, such as air inlet/outlet and window, can be considered as a sharp orifice that their C_d are considered as the same [48]. The volumetric flow rate through a sharp orifice can be given by,

$$V_j = C_d A_j U_j \tag{3}$$

where V is the volumetric flow rate through the orifice, m^3/s; C_d is the coefficient of discharge; and A is the area of the orifice, m^2.

It is indicated in Fig. 2(b) that the P_{i1} is higher than P_{w2}. The airflow from the window enters the cavity through the air inlet under the initial velocity at the window. The related experimental and numerical results [49,50] have proved this. The following relationship can be given between these two,

$$P_{i1} - P_{w2} = \rho_r g H_w \tag{4}$$

where P_{i1} and P_{w2} are the gas pressure near the air inlet and window, as shown in Fig. 2, Pa; r represents the room; and H_w is the height of window centre to the floor, m.

The relationship between P_{o2} and P_{w1} shown in Fig. 2(b) can be obtained following Eq. (1). For the pair pressures of P_{w1} and P_{w2}, the relationship shown in Eq. (2) is applicable for pressure gradient at the two sides of the orifice. As the heating source in the room is considered minimal, the temperatures inside the room and outside are almost the same. Based on this series of equations, it is obtained,

$$\rho_0 U_w^2 + \rho_r U_i^2 + \rho_c U_o^2 = 2(\rho_0 - \rho_c) g H_c \tag{5}$$

where ρ_0, ρ_r, and ρ_c represents the air density in the ambient, the room and chimney cavity, respectively, kg/m^3; U_w, U_i and U_o are the airflow velocities through the window, air inlet and outlet, respectively, m/s; and H_c is the height of chimney cavity between the cavity top and the floor, m.

Under the steady conditions, the air flow inside the room and the cavity are stable along the time. The mass fluxes through the inlet and outlet are considered equal for each chamber. Based on this, the mass conservation equation can be given by,

$$\rho_c V_o = \rho_r V_i = \rho_0 V_w \tag{6}$$

All the velocities through the orifices can be converted to volumetric flow rate based on Eq. (3). And Eq. (5) can be rearranged

after replacing V_i (also V_w) with V_o through Eq. (6),

$$V_o = C_d\sqrt{\frac{2A_w^2A_i^2A_o^2(\rho_0-\rho_c)gH_c}{\left(\frac{\rho_c}{\rho_0}A_i^2A_o^2+\frac{\rho_c}{\rho_r}A_w^2A_o^2+A_w^2A_i^2\right)\rho_c}} \tag{7}$$

Following the assumption that there is a minimal heat source in the room, so it can be assumed $\rho_r = \rho_0$. Usually, it is also assumed that $\rho_c = \rho_0 = \rho_r$ in the denominator of the right-hand side of Eq. (7). Therefore, Eq. (7) can be simplified as,

$$V_o = C_dA_r^*\sqrt{\frac{(\rho_0-\rho_c)gH_c}{\rho_c}} \tag{8}$$

where A_r^* represents the coefficient for solar chimney considering room configuration,

$$A_r^* = \sqrt{\frac{2A_wA_iA_o}{A_iA_o+A_wA_o+A_wA_i}} \tag{9}$$

The ideal gas law can be simplified with a less than 0.02% error within the practical application temperature range, and it is given by Ref. [41]:

$$\rho_cT_c = \rho_rT_r = \rho_0T_0 \tag{10}$$

where T_c, T_r, and T_0 represent the temperature at the chimney cavity, room and the ambient, respectively, K.

Based on Eq. (10), the volumetric flow rate at the outlet, as shown in Eq. (8), can be given by,

$$V_o = C_dA_r^*\sqrt{\frac{(T_c-T_0)gH_c}{T_0}} \tag{11}$$

Under the steady conditions, the temperature inside the chimney cavity keeps constant (or balanced) along the time. The solar energy penetrated through the glazing wall is basically used to heat the incoming air to the balanced temperature inside the cavity. The energy conservation equation for chimney cavity under steady conditions is expressed by,

$$E_c = \rho_cV_oC_p(T_c-T_r) \tag{12}$$

where E_c is the power of heating intensity in the chimney cavity, W; and C_p is the specific heat capacity of the air, J/kg·K.

In Eq. (12), a further assumption of $\rho_r = \rho_0$ and $T_r = T_0$ is just a compensation of the previous assumption during the development A_r^*. It was also tried to solve the equation group without these assumptions, while the same analytical solution can be obtained after getting rid of the terms which can be ignored. Based on Eqs. (11) and (12), the volumetric flow rate at the outlet of solar chimney considering room configuration can be given by,

$$V_o = \left(C_dA_r^*\right)^{\frac{2}{3}}(BH_c)^{\frac{1}{3}} \tag{13}$$

where B is the buoyancy flux, which is the driven force of the flow inside the chimney cavity,

$$B = \frac{E_cg}{\rho_0C_pT_0} \tag{14}$$

2.2. Fresh-air heating through cavity

Solar chimney under fresh-air heating through the cavity can be seen in Fig. 3(a). It is similar to the cooling mode, while the air is not exhausted to the outside but the indoor environment. The chimney cavity is evenly heated through the vertical glazing wall by solar radiation, while the internal air can be considered well mixed with uniform air density (ρ_c) and temperature (T_c). As the hot air at the upper layer of room sources from the chimney cavity, its temperature and density can be considered well mixed, with a uniform temperature and air density of T_r and ρ_r, respectively. The lower layer of the air inside the room is ambient air (T_0 and ρ_0).

For the well-mixed air, its hydrostatic pressure is linear to the height from the floor, showing a changing rate of ρg. Based on this, the pressure distributions inside both chimney cavity and the room could be three possible scenarios,

- In Fig. 3(b), this is an unsteady scenario. At the beginning, the interface of the hot air is higher than the top boundary of the window, while the window is purely for the exhaustion of the ambient air from the room. When the interface keeps dropping and is lower than the top boundary of the window, the upper part of the window starts to exhaust hot air and the lower part to exhaust ambient air from the room;
- Fig. 3(c) shows a steady scenario. This happens when the interface of the hot air is aligned with the heights of the window and neutral plane. Gas pressures at outdoor and inside the room keep increasing downwards. After the convergence of these two pressure curves, the increasing rates become the same when both are within the ambient air. Under the condition, the upper part of the window is for the exhaustion of hot air. There is very limited air exchange at the lower part of the window, which is because the mass of the lower part of ambient air inside the room should keep the same under the steady conditions. Under a strong plume (e.g. fire plume [51,52]), the situation may be different, which is beyond the scope of this study; and
- An unlikely scenario is shown in Fig. 3(d). Under this condition, the upper part of the window is used for the exhaustion of the hot air, while the lower part is for the entry of ambient air from the outdoor environment. This is inconsistent with the pressure distribution for the upper window. For the room below the junction of pressure curves, filled with the ambient air, the increasing rate of the pressure along the height should follow that of the outdoor environment but not the hot air. Namely, these two pressure curves should coincide with each other for the height below the neutral plane (H_{n2}), similar to Fig. 3(c).

According to the above analysis, it is known that the window under the circumstance is used or partly used for the exhaustion of the hot air under steady condition. For a small window with limited height, the whole window may be used for the exhaustion of the hot air. With a relatively big window, its lower part may not be used for the exhaustion of hot air, but there is a limited exchange of ambient air between the room and outdoor environment under a limited pressure gradient.

Under the steady conditions, the airflow through the window can be simply considered as a unidirectional flow, namely the whole window can be considered as the exhaustion of the hot air with a total airflow denoted by V_w, represented by Fig. 3(c). The pressure difference at various heights can be given by,

$$P_{i2} - P_{o1} = \rho_cgH_c \tag{15}$$

$$P_{o2} - P_{w2} = -\rho_r g(H_c - H_w) \tag{16}$$

$$P_{i1} - P_{w1} = \rho_0 g H_w \tag{17}$$

As the hot air at the upper part of the room sources from the chimney cavity and the heating source inside the room is limited, its air density can be considered as the same with that inside the chimney cavity. After combining Eqs. (15) to (17), it is known that,

$$\rho_0 U_i^2 + \rho_c U_o^2 + \rho_r U_w^2 = 2(\rho_0 - \rho_c) g H_w \tag{18}$$

According to the mass conservation of both chimney cavity and the whole domain (chimney cavity and the room), a relationship can be determined as,

$$\rho_0 V_i = \rho_c V_o = \rho_r V_w \tag{19}$$

Based on the above Eqs. (18) and (19) and the theory for volumetric flow rate through a sharp orifice as shown in Eq. (3), the volumetric flow rate at the outlet of the chimney cavity can be given by the temperature difference from the ambient air,

$$V_o = C_d A^* \sqrt{\frac{g(T_c - T_0) H_w}{T_0}} \tag{20}$$

where A^* is the coefficient related to the areas of all the openings,

$$A^* = \frac{2A_i^2 A_o^2 A_w^2}{A_o^2 A_w^2 + A_i^2 A_w^2 + A_i^2 A_o^2} \tag{21}$$

The glazing wall of the chimney cavity allows solar penetration to heat up the internal air. Under the steady status, the temperature of internal air keeps constant, while the absorbed heat is used to heat the fresh air to the temperature of the hot air. Based on energy conservation, the following relationship can be obtained,

$$E = \rho_c V_o C_p (T_c - T_0) \tag{22}$$

After combining Eqs. (20) and (22), the volumetric flow rate at the outlet of the chimney cavity can be given by,

$$V_{out} = \left(C_d A^*\right)^{2/3} (B H_w)^{1/3} \tag{23}$$

where B is the buoyancy flux, which is represented in Eq. (14).

Based on Eqs. (22) and (23), the temperature of the air inside the chimney cavity can be obtained by,

$$T_c = \left(\frac{T_0}{g H_w}\right)^{1/3} \left(\frac{E}{\rho_0 C_p C_d A^*}\right)^{2/3} + T_0 \tag{24}$$

As the volumetric flow rate at the outlet is constant under a constant solar radiation. The time to achieve the steady status, when the hot air layer approaches the window, can be simply calculated by the volume of the upper part of the room and volumetric flow rate,

$$t_{ste} = \frac{A_r (H_c - H_w)}{(C_d A^*)^{\frac{2}{3}} (B H_w)^{\frac{1}{3}}} \tag{25}$$

where t_{ste} represents the time to achieve the steady status of the airflow, s; and A_r is the floor area of the room, m^2.

Before the hot air layer arrives at the window height, namely the time is less than t_{ste} obtained by Eq. (25), the height of the hot layer in the room from the floor, H_{hot}, can be then estimated by,

$$H_{hot} = max\left[H_c - \frac{t(C_d A^*)^{2/3} (B H_w)^{1/3}}{A_r}, H_w\right] \tag{26}$$

where H_{hot} is the height of the hot air interface in the room from the floor, m; and t is the time since the beginning of the heating process, s.

It should be mentioned that the room opening in the above analysis is not only applicable to window but also door. Eq. (23) is applicable to multiple vertical openings such as window and door due to the mass balance in the whole domain and the openings can exhaust the upper hot air layer after the interface keeps dropping.

2.3. Fresh-air heating through room

Solar chimney under fresh-air heating through the room, as shown in Fig. 4(a), is similar to the second type. The difference is that the fresh air supply is through the room opening (e.g. window or door). Based on the mass conservation of the whole domain (both chimney cavity and room), the total mass flow through the room opening should be equal to zero under steady status, which is similar to those rooms under single-sided natural ventilation [53]. This can be described by two stages. At the first stage, hot air exhaust to the room from the chimney cavity after been heated. Before they approach the window top, the room opening is only used for the exhaustion of the ambient air inside the room. After the hot air layer approaching the window height, denoted as the second stage, the window starts to exhaust hot air due to the pressure gradient, while the lower part of the window is then used for fresh air supply.

Fig. 4(b) shows the pressure distributions of outdoor, the room and chimney cavity. The window can be also divided into two parts, while at the upper part $P_{w2}>P_{w1}$ and the lower part $P_{w3} = P_{w4}$. For the upper part of the window, the hot air can be exhausted under the pressure gradient. The lower part is different from Fig. 3(c) even though both the pressure gradients are zero. This is because the ambient air at the lower part of the room enters the chimney cavity through the air inlet under the pressure gradient. After that, the outdoor fresh air enters the room through the lower part of the window to compensate for the loss of the ambient air under the steady status. This is the reason why the lower part of the window still exists an incoming fresh air even though the pressure gradient is zero.

According to the mass conservation of the chimney cavity under steady status, the mass fluxes at the inlet and outlet are the same. Similar for the lower layer inside the room, namely the ambient air layer, the mass of fresh air flowing into the room from the outside environment is equal to that entering the chimney cavity from the room, as the interface between the hot air and ambient air keeps unchanged under steady status. The neutral plane (H_n) is located within the window, whatever the height of the window is. If we assign V_{uw} and V_{lw} the upper entering and lower outgoing volumetric flow rates, respectively, it is then known that,

$$\rho_c V_o = \rho_r V_{uw} \tag{27}$$

$$\rho_0 V_{lw} = \rho_0 V_i \tag{28}$$

where V_{uw} and V_{lw} are the air flow volume through the upper and lower part of the window, m^3/s.

Under the steady status of the chimney cavity, it is obtained that $\rho_0 V_i = \rho_c V_o$, so the following expression can be determined,

$$\rho_0 V_{lw} = \rho_r V_{uw} \tag{29}$$

Previous studies [54,55] assumed that for a room with single-sided natural ventilation half of the opening is used for entering airflow and another half for exhaustion. This study will follow the same assumption under the similar situation. According to the pressure distributions inside the chimney cavity, the room, and outdoor environment, as shown in Fig. 4(b), the pressure differences can be obtained as,

$$P_{i2} - P_{o1} = \rho_c g H_c \tag{30}$$

$$P_{o2} - P_{w2} = -\rho_r g(H_c - H_w - 0.25h_{s,w}) \tag{31}$$

$$P_{w1} - P_{w4} = -0.5\rho_0 g h_{s,w} \tag{32}$$

$$P_{i1} - P_{w3} = \rho_0 g(H_w - 0.25h_{s,w}) \tag{33}$$

where $h_{s,w}$ is the size (or called vertical height from its bottom to the top) of the window, m;

For the window with both entering and outgoing air flows, the discharge coefficient can still be applied even this is not strictly a vena contracta as the discharge coefficient can account for streamline contraction and viscous loss incurred through the opening [56,57]. So the calculations of P_{w2}-P_{w1} and P_{w4}-P_{w3} can still follow Eq. (2).

Based on Eqs. (30)–(33), it is known that,

$$\rho_0 U_i^2 + \rho_c U_o^2 + \rho_r U_{uw}^2 + \rho_0 U_{lw}^2 = 2(\rho_0 - \rho_c) g(H_w + 0.25h_{s,w}) \tag{34}$$

It is also known from Eqs. (27) to (29) that,

$$\rho_0 V_i = \rho_c V_o = \rho_r V_{uw} = \rho_0 V_{lw} \tag{35}$$

The energy conservation equation is the same with previous chimney type, as shown in Eq. (22). After combining Eqs. (3), (22), (34) and (35), the volumetric flow rate at the outlet of the chimney cavity can be expressed by,

$$V_o = \left(C_d A^*\right)^{2/3} \left[B(H_w + 0.25h_{s,w})\right]^{1/3} \tag{36}$$

where B is the same with Eq. (14), but A^* is different from that in Eq. (21), which can be given by,

$$A^* = \sqrt{\frac{2A_i^2 A_o^2 A_w^2}{A_o^2 A_w^2 + A_i^2 A_w^2 + 8A_i^2 A_o^2}} \tag{37}$$

The temperature of the air inside the chimney can be estimated by,

$$T_c = \left[\frac{T_0}{g(H_w + 0.25h_{s,w})}\right]^{1/3} \left(\frac{E}{\rho_0 C_p C_d A^*}\right)^{2/3} + T_0 \tag{38}$$

Similarly, the time to approach steady status when the hot air layer approach the window height and the hot layer height inside the room can be given by, respectively,

$$t_{ste} = \frac{A_r(H_c - H_w)}{\left(C_d A^*\right)^{2/3} \left[B(H_w + 0.25h_{s,w})\right]^{1/3}} \tag{39}$$

$$H_{hot} = max\left[H_c - \frac{t\left(C_d A^*\right)^{2/3} \left[B(H_w + 0.25h_{s,w})\right]^{1/3}}{A_r}, H_w\right] \tag{40}$$

2.4. Sealed heating

Fig. 5(a) shows the solar chimney under sealed heating. As can be seen in this figure, no fresh air enters the domain through the room neither the chimney cavity. After the air been heated through the chimney cavity, the hot air exhaust to the room and gather at the ceiling under thermal buoyancy. Along the process, the interface between the upper hot air and lower ambient air keeps dropping until it touches the floor. This is the time the whole room space is heated, when it can be considered achieving the steady status, even though there might be slight air movement under the limited temperature difference. The air flow finally stops moving when there is a heat balance that the absorbed heat of the air inside the chimney cavity is equal to their radiation heat to the surrounding environment.

Therefore, the theoretical analysis for sealed heating should focus on the dynamic (unsteady) heating process, which is different from the previous three types. The pressure distribution can be seen in Fig. 5(b). Those pressure differences at various heights along the time under unsteady conditions are similar to Eqs. (15) to (17) or Eqs. (30) to (33).

Following the similar deduction as the previous two types, the dynamic volumetric flow rate can be obtained as,

$$V_o = \left(C_d A^*\right)^{2/3} (BH_{hot})^{1/3} \tag{41}$$

where B is the same with Eq. (14) and A^* is expressed as,

$$A^* = \frac{2A_i^2 A_o^2}{A_i^2 + A_o^2} \tag{42}$$

As the hot air from the chimney cavity fills the upper part of the room, a relationship can be then determined between the dynamic V_o and H_{hot},

$$\frac{\partial(H_c - H_{hot})}{\partial t} = \frac{V_o}{A_r} \tag{43}$$

After combining Eqs. (41) and (43), it is known,

$$\frac{\partial H_{hot}}{\partial t} = -\frac{\left(C_d A^*\right)^{2/3} (BH_{hot})^{1/3}}{A_r} \tag{44}$$

Separating the variables and integrating both sides, Eq. (44) can be rewritten as,

$$\int H_{hot}^{-\frac{1}{3}} \partial H_{hot} = \int -\frac{\left(C_d A^*\right)^{2/3} B^{1/3}}{A_r} \partial t \tag{45}$$

So the dynamic height of the hot layer can be given by,

$$H_{hot} = \left[\frac{2}{3}C - \frac{2\left(C_d A^*\right)^{2/3} B^{1/3}}{3A_r} t\right]^{3/2} \tag{46}$$

where C is the constant, which can be obtained through the initial conditions. When $t = 0$, $H_{hot} = H_c$. Based on this, it is obtained that $c = \frac{3}{2}H_c^{2/3}$. So,

$$H_{Hot} = max\left\{\left[H_c - \frac{2tB^{1/3}\left(C_d A^*\right)^{2/3}}{3A_r}\right]^{3/2}, 0\right\} \tag{47}$$

As the accumulation of the upper hot air layer continues, H_{hot} drops and approaches the floor. The time needed for the hot air filling the whole room space is when $H_{hot} = 0$. The time for the solar chimney to heat the whole room space can be estimated by,

$$t_{ste} = \frac{3A_r H_c}{2B^{1/3}(C_d A^*)^{2/3}} \tag{48}$$

So, the air movement inside the chimney cavity stops only when the internal temperature is stable. This is the time when there is a heat balance between the absorbed heat from the solar radiation and the radiation heat from the internal air to the surrounding environment. To obtain the temperature of the air inside the chimney cavity, several main thermal processes should be considered, such as transmission of solar radiation for the glazing wall, radiation heat, and convective heat among three surfaces (e.g. glazing wall, internal air and the absorption wall). The energy conservation equation for the air inside the chimney cavity is given by:

$$\rho_a C_p V \frac{\partial T_c}{\partial t} = \tau\mu_a A_c Q_{sol} - A_c\sigma\left(T_c^4 - T_0^4\right) - A_c h_a(T_c - T_a) - A_c h_{wall}(T_c - T_{wall}) \tag{49}$$

where Q_{sol} is the solar radiation intensity, W/m^2; V here is the volume of the chimney cavity, m^3; τ is the transmissivity of glazing; A_c is the area of the absorption (or hot) wall, m^2; μ_a is the absorption coefficient of the air; σ is the Stefan-Boltzmann constant, W/m$^2\cdot$K^4; and h_{wall} is the heat transfer coefficient of the wall, W/m$^2\cdot$K.

When it approaches the steady status, the term on the left-hand side is equal to zero,

$$\tau\mu_a Q_{sol} - \sigma\left(T_c^4 - T_0^4\right) - h_a(T_c - T_a) - h_{wall}(T_c - T_{wall}) = 0 \tag{50}$$

Under the steady status, it is considered that $T_c = T_a = T_{wall}$, so the temperature of the internal air can be estimated by,

$$T_c = \left(\frac{\tau\mu_a Q_{sol}}{\sigma} + T_0^4\right)^{1/4} \tag{51}$$

2.5. Effects of room configuration

In this section, the solar chimney under cooling mode was used as an example to show the influence of the connected room on the performance. Based on Eq. (13), it can be seen for a typical wall solar chimney under cooling mode that the influences of the connected room are much reflected by the room opening area. A_r^* in Eq. (13) can be also given by,

$$A_r^* = \sqrt{\frac{2A_i^2A_o^2}{\frac{1}{A_w}A_i^2A_o^2 + \left(A_o^2 + A_i^2\right)}} \tag{52}$$

In the above equation, if $A_w \to \infty$, $A_oA_i/A_w \to 0$ that the dominator of the right side term is equal to $A_o^2 + A_i^2$, so $A_r^* = A_c^*$, where A_r^* and A_c^* represent the coefficient for solar chimney considering and without considering room configuration, respectively. It is indicated if there is an infinite big opening for the connected room, the volumetric flow rate is equal to the solo solar chimney without considering room configuration,

$$A_c = \sqrt{\frac{2A_i^2A_o^2}{A_o^2 + A_i^2}} \tag{53}$$

The infinitely big opening of the room can be considered as the scenario that the solar chimney is directly connected to the ambient environment without going through a room, when the solar chimney achieves the maximum performance. A room coefficient, ζ, is then proposed to present the percentage of solar chimney performance to its maximum performance,

$$\zeta = \frac{V_{o,r}}{V_o} \tag{54}$$

where $V_{o,r}$ and V_o are the volumetric airflow rate through the chimney cavity connecting a room and directly the ambient environment, respectively, m^3/s.

Based on Eqs. (13), (52) and (53), the room coefficient can be expressed by,

$$\zeta = \left(\frac{A_r^*}{A_c^*}\right)^{\frac{2}{3}} = \left[1 + \frac{1}{(A_w/A_i)^2 + (A_w/A_o)^2}\right]^{-\frac{1}{3}} \tag{55}$$

Eq. (55) further proves that if $A_w \to \infty$, $\zeta = 1$, where the solar chimney performance achieves the maximum with a room coefficient of 100%. So if we want the solar chimney performance achieves a specific ζ, the room opening should be bigger than a specific area, which is given by,

$$A_w > \left[\left(\zeta^{-3} - 1\right)(A_i + A_o)\right]^{-0.5} \tag{56}$$

Fig. 6(a) shows an example of determining the minimal area of room opening when it is connected to a solar chimney with a 0.3 m high air inlet with a cavity depth of 0.05–0.3 m. It can be seen from this figure that the increasing rate of ζ drops with a bigger room opening area. For example, for the chimney cavity with a depth of 0.05 m, ζ increases from 47% to 68% when opening area rises from 0.05 to 0.10 m^2. However, after that, the same increase of ζ needs a rise of the opening area from 0.10 to 0.23 m^2. The same situation applies to Fig. 6(b) with various cavity widths. It can be seen from Eq. (56) that the cavity height shows limited influence on the required room opening.

For this solar chimney under cooling mode, if we need to achieve a room coefficient of 90%, the required room opening area varies from 0.25 to 1.05 m^2 dependent on the cavity depth. For the solar chimney with 0.3 m cavity depth, the minimal area of the room opening is about 1.05 m^2. A regularly adopted half-open window (1.2 m × 1.8 m) could be enough to achieve a room coefficient of 90%. But if we increase the cavity depth or width, this typical window is then not enough.

3. Validations of theoretical models

Solar chimney is different from solar photovoltaic which produces electricity directly, while the energy saving of the target building is realized by promoting natural ventilation and saving the

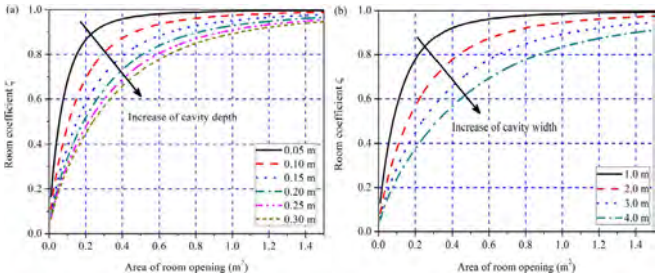

Fig. 6. Relationship between the room coefficient and room opening area for a solar chimney with a 0.3 m high air inlet under various: (a) cavity depths (0.05–0.3 m); and (b) cavity widths (1.0–4.0 m).

energy which is originally consumed by HVAC system. Under the circumstance, the higher airflow rate raised by the chimney cavity the better performance of solar chimney is. At the moment, very limited studies have been found for solar chimney connected to a room under cooling mode, not to mention the heating mode. Two experimental studies have been found in the literature regarding the cooling mode, while one is an outdoor test and the other is indoor. In this section, the experimental data about the volumetric airflow rate through the solar chimney were utilized to validate the theoretical model under cooling mode, while the validation of heating mode will be taken in our future work when the experimental data are available. As the airflow rate through the solar chimney is one of the key parameters to determine its performance, the airflow rates through the chimney cavity between the numerical modeling and experiments were then compared for the validation.

3.1. Outdoor experiment

An outdoor test was undertaken by Mathur et al. [58]. The test rig was briefly introduced here for convenience and completeness, while more details can refer to the reference. A reduced-scale test rig of 1 m cubical room was built with timber and connected to a solar chimney. On the right side of the room, a 0.5 m high opening (window) was built with a dimension of 0.3 m × 0.3 m for fresh air supply. The structure of the room and solar chimney can refer to Fig. 2(a).

An absorber wall was positioned between the chimney cavity and the room, which can be adjusted vertically for parametric analysis. The left side of the absorber wall was attached with a 1 mm black pained aluminum sheet to enhance the solar absorption, while its right was placed with 5 cm insulation to minimize the heat transfer from the cavity to the room. Its height can be adjusted during experiment within a range of 0.7–0.9 m under 0.1 m increment, leaving an air inlet height of 0.3–0.1 m. A glazing wall was located at the left side of the cavity, allowing solar penetration. The distance between glazing and absorber wall, called cavity depth, was adjustable between 0.1 and 0.3 m under 0.1 m increment.

The temperatures of the absorber wall, glazing and airflow in the chimney cavity were measured by K-type thermocouples. Airflow velocity was measured by a hot-wire anemometer with an accuracy of 0.01 m/s. The anemometer wire was located 15 cm below the outlet and in the middle of glazing and absorber walls. The solar radiation was measured parallel to the absorber wall by a solarimeter with least-count 15 W/m^2 and accuracy of ±1%. All the measurements were taken under three solar intensities, namely 300, 500 and 700 W/m^2. To reduce the influences from outdoor wind, a blocking wall was built 0.5 m from the window with a dimension of 3 m (width) × 2 m (height). All the measurements were taken under minimal wind with a velocity of less than 0.1 m/s.

The inputted values for the prediction are listed in Table 1. A comparison between experimental and predicted airflow rate can be seen in Fig. 7. The predictions are based on two methods: (a) traditional way (without considering room configuration), as shown in Eq. (53) [45]; and the proposed theoretical model in this study (considering room configuration). It can be seen from the comparison that the predictions without considering room configuration are higher than the experimental data, showing an average error of 49.0%. The predicted flow rates, based on the proposed model in this study after considering the room configuration, are much improved, showing an average error of 25.2%. It can be then known that the room configuration shows considerable influences on the airflow rate through solar chimney.

Although an average error of 25.2% is still obvious, this may be because of the unstable test environment in the outdoors. According to the experiments, the maximum air velocity inside the chimney cavity is about 0.33 m/s. As mentioned in the literature, all the readings were taken when the external wind is less than 0.1 m/s, which can also provide an unneglectable impact on the experimental measurement. This may be the reason why there is still an average error of 25.2% after considering the connected room. Although the differences between the experiment and prediction cannot be ignored, it positively shows that the consideration of the room configuration can provide much practical/improved predictions for the design of solar chimney.

Table 1
A summary of inputted values for the prediction.

Symbol	Meaning	Value	Unit	Reference
C_d	Coefficient of discharge	0.57	–	[58]
C_p	Specific heat capacity of air	1005	J/kg·K	[59]
h	Heat transfer coefficient	15	W/m^2·K	[49]
ε	Emissivity	0.96	–	[60]
ρ_0	Ambient air density	1.205	kg/m^3	[59]
σ	Stefan-Bolzmann constant	5.6704×10^{-8}	W/m^2·K^4	[61]
τ	Transmissivity of glazing	0.74	–	[58]

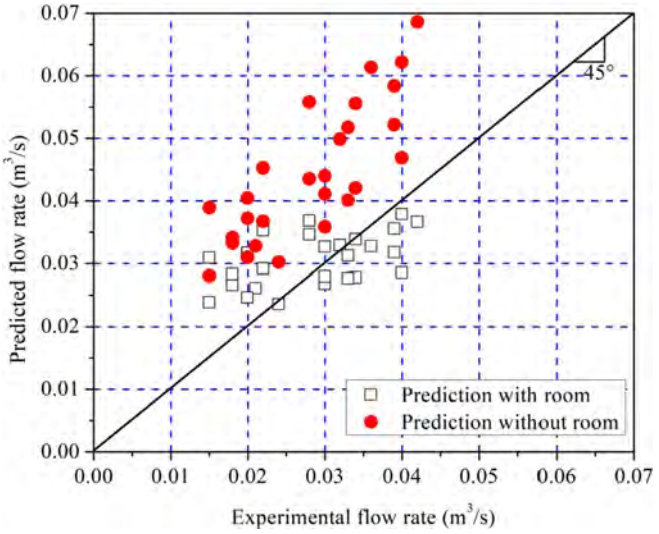

Fig. 7. A comparison of experimental and predicted airflow rate through chimney cavity. The experimental data come from Ref. [58].

For this experimental setup, the area of room opening keeps at 0.09 m^2, while the areas for air inlet and outlet are both within 0.1–0.3 m^2. According to Eq. (55), the maximum room coefficient can be achieved when the areas of the inlet and outlet are both at 0.1 m^2, which is 85%. However, when both areas increase to 0.3 m^2, the current window is not enough to sustain a high performance that the room coefficient drops from 85% to 53%. It is suggested to have a room opening (window or door) of no less than 0.35 m^2 to keep an over 90% room coefficient for this experimental setup.

3.2. Indoor experiment

The indoor experiment was conducted by Bouchair [62] in a large enough laboratory (20 m long × 10 m wide × 5 m high). The ambient air temperature was kept at 20 °C. The structure of the test room is the same as Fig. 2(a), including a room and a chimney cavity. The room was made of timber with an internal dimension of 1.8 m (L) × 1.65 m (W) × 2.0 m (H). An opening (or window) was considered at the centre of the right wall with a dimension of

0.5 m (W) × 0.6 m (H). The air inlet of the chimney cavity is 1.4 m wide with two heights (0.1 and 0.4 m).

Different from the previous outdoor test model, the two walls constructing chimney cavity were made of insulation board, attached with polished aluminum on the cavity side to benefit the reflection of heating source. The dimension of the chimney cavity is 1.5 m (W) × 2.0 m (H) with various depths of 0.1–1.0 m. The heating process is also different from the outdoor test, which was realized by two electrically heated panels, providing a wall temperature of 30–60 °C. Several controllers were utilized to ensure the surface temperature of the panels was kept at the designed one. The air flow and temperature of multiple points at the air inlet were measured by heated thermistor anemometer with an accuracy of ±5% velocity reading and ±1 °C temperature, respectively.

During the experiment, the two walls constructing the chimney cavity were first heated to the target temperature. Air velocities were monitored to determine if the air flow is stable. Fluctuations were observed high under the variability of the airflow. Both the temperature and velocity for the individual scenario were averaged values during a period of 90 s. More details about the test rig and measurement procedure can be seen in Ref. [62].

As the heating source in the experiment was represented by the hot wall, it is needed to convert the temperature to heating power (or called solar radiation intensity) for the modeling input of the theoretical models. The total heating power is determined by a combination of convective and radiation heat transfer between the hot wall and the surrounding air. A direct calculation seems to be impossible as the temperature of internal air is not known and changing along the time. It can be known that for a temperature range of 30–80 °C, the normal application range for solar chimney, radiation heat flux is about 33.8 ± 4.2% of the convection heat flux between the hot wall and ambient air. Therefore, for simplification, the heating power of the hot wall was obtained based on the convective heat transfer between the hot wall and ambient air.

The predictions considering and without considering the room configuration can be seen in Fig. 8. These predictions are based on the inputs listed in Table 1. The same with the outdoor test, it can be observed that the predictions considering room configuration are much improved. The average error of predictions drops from 41.0% to 17.5% after considering the room configuration. When comparing to the outdoor prediction, the predictions for the indoor test are much better with an average error of about 7.7%. It may prove that the errors for the predictions of the outdoor test are because of the external unstable environment such as external wind. The errors still exist after considering the room, as seen in Fig. 8, which may because of the simplified calculation method for the total heat flux.

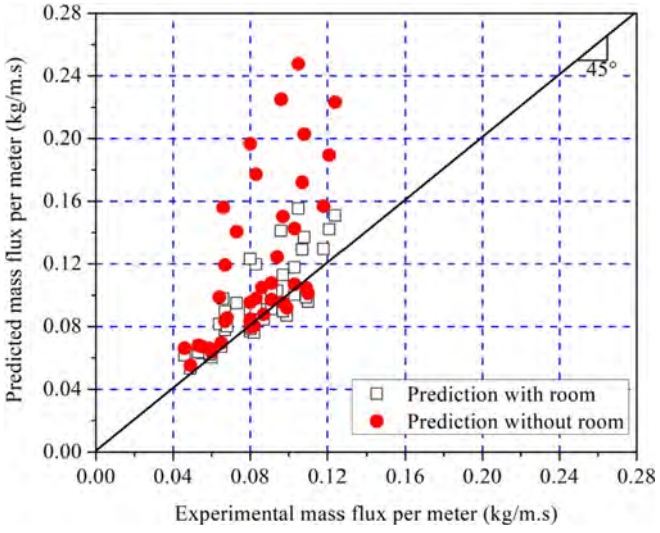

Fig. 8. A comparison between experimental and predicted mass flux per meter. The experimental data come from Ref. [62].

So based on the above outdoor and indoor experiments, it can be seen that the influences of the room configuration on solar chimney performance cannot be ignored and the proposed theoretical model in this study can provide much accurate predictions for the solar chimney.

4. Comparisons and implementations

4.1. Comparisons among four types

Based on the above analysis, theoretical models were developed to predict the volumetric flow rate and the temperature of the chimney cavity. A summary of these theoretical models can be seen in Table 2. The comparisons are made among four typical types of solar chimney, including cooling mode and three heating modes, in terms of volumetric flow rate through the chimney cavity (V_o), temperature of hot air (T_c), time to achieve steady status (t_{ste}), and height of hot layer from the floor (H_{hot}).

It can see from Table 2 that the theoretical models of volumetric flow rate show exactly the same format for these four categories, but with different A^* and H. The coefficient A^* is a little different for sealed heating as there is no opening for both chimney cavity and the room. Due to the function of the window, A^* is a little different for fresh-air heating through the room. For solar chimney under cooling mode, the H is the height of cavity/chimney, while under heating mode it is much related to the height or size of the window. Except for the sealed heating category, the other three types show stable volumetric flow rate along the time. As the volumetric flow rate under sealed heating is dependent on the height of the hot air layer, the volumetric flow rate keeps decreasing when the hot layer approaches the floor.

As shown in Eq. (22), the temperature of the hot air is much dependent on the volumetric flow rate. Under the fixed heat input (solar radiation), a larger airflow rate means more air is heated, which then results in a relatively lower temperature of the hot air through the chimney cavity. The calculation of the temperature under sealed heating is different from the other three types as the volumetric flow rate keeps decreasing along the time before it fills the whole room space. The calculation of the temperature is then based on the energy conservation of absorbed solar radiation and the emitted radiation heat of the hot air inside the chimney cavity, as shown in Eqs. (49) and (50). This is the reason why the obtained temperature of the hot layer for the type of sealed heating is a little different from the others.

The time to achieve steady status is a little different for solar chimney under sealed heating as the hot air layer can touch the floor, while for the other three types only approach the window centre. So the time to achieve steady status for solar chimney under sealed heating is the time when the hot air layer touches the floor, with the double travel distance than the others. The height of the hot air layer is dependent on the volumetric flow rate of the hot air through the chimney cavity and the floor area. For a fixed floor area, a bigger volumetric flow rate is companied with a more rapidly descendent hot layer.

For a typical building, the advantages and disadvantages of solar chimney for the heating purpose can be seen in Table 3. It is known that except sealed heating, the other two types allow the fresh-air exchange to the outdoor environment. The fresh-air heating through cavity show averagely the highest air exchange rate and the lowest temperature and fresh-air heating through the room is

Table 2
A summary of developed theoretical models for solar chimney.

Category	Schematic	Theoretical models	Note
Cooling	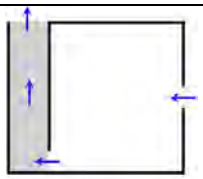		$A^* = \frac{2A_i^2 A_o^2 A_w^2}{A_o^2 A_w^2 + A_i^2 A_w^2 + A_i^2 A_o^2}$ $H = H_c$
Fresh-air heating through cavity	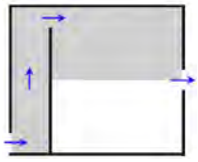	$V_o = \left(C_d A^*\right)^{2/3} (BH)^{1/3}$ $T_c = \left(\frac{T_0}{gH}\right)^{1/3} \left(\frac{E}{\rho_0 C_p C_d A^*}\right)^{2/3} + T_0$ $t_{ste} = \frac{A_r (H_c - H_w)}{\left(C_d A^*\right)^{2/3} (BH)^{1/3}}$	$A^* = \frac{2A_i^2 A_o^2 A_w^2}{A_o^2 A_w^2 + A_i^2 A_w^2 + A_i^2 A_o^2}$ $H = H_w$
Fresh-air heating through room	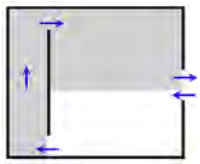		$A^* = \frac{2A_i^2 A_o^2 A_w^2}{A_o^2 A_w^2 + A_i^2 A_w^2 + 8A_i^2 A_o^2}$ $H = H_w + 0.25 h_{s,w}$ $H_{hot} = max\left[H_c - \frac{t\left(C_d A^*\right)^{2/3} (BH)^{1/3}}{A_r}, H_w\right]$
Sealed heating	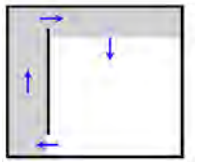	$V_o = \left(C_d A^*\right)^{2/3} (BH)^{1/3}$ $T_c = \left(\frac{\tau \mu_a Q_{sol}}{\sigma} + T_0^4\right)^{1/4}$ $t_{ste} = \frac{3A_r H_c^{2/3}}{2B^{1/3}\left(C_d A^*\right)^{2/3}}$	$A^* = \frac{2A_i^2 A_o^2}{A_i^2 + A_o^2}$ $H = H_{Hot} = max\left\{\left[H_c^{2/3} - \frac{2tB^{1/3}\left(C_d A^*\right)^{2/3}}{3A_r}\right]^{3/2}, 0\right\}$

Note: V_o is the volumetric flow rate at the outlet; C_d is the coefficient of discharge, which is normally considered as around 0.6 for door and window [48]; A_i is the inlet area; A_o is the outlet area; A_w is the room opening area; A_r is the floor area of the room; H_c is the height of the chimney cavity or room ceiling; H_w is the distance between room opening centre and the floor; H_{hot} is the height of the hot layer bottom interface from the floor; t is the time started from the beginning; B is the buoyancy flux, which can be obtained through Eq. (14); T_c is the air temperature inside chimney cavity or the hot layer inside the room; T_0 is the ambient air temperature; C_p is the specific heat capacity of ambient air; ρ_0 is the ambient air density; E is the heat absorbed by the air inside the chimney cavity, which can be estimated by $A_r \tau Q_{sol}$; τ is the transmissivity of glazing wall of solar chimney; Q_{sol} is the solar radiation intensity; $h_{s,w}$ is the height of room opening itself from its top to bottom frames; g is the acceleration of gravity; and μ_a is the absorption coefficient of the air.

in an opposite way, while the sealed heating shows a moderate performance in terms of both airflow rate and temperature. Fresh-air heating through cavity can heat the upper room quite faster than the fresh-air heating through the room. Therefore, it is suggested to use fresh-air heating through the cavity, through the room and sealed heating to regularly occupied buildings under cool and cold weather conditions, and non-regularly occupied buildings (e.g. storages), respectively.

4.2. Implementation of models

To implement the theoretical models developed in this study, a typical room with an area of 36.0 m^2 and a height of 2.7 m was selected. For the two types with window, a typical half-closed sliding window with a dimension of 1.2 m (height) × 1.8 m (width) is located in the middle of the right wall. The area of the real opening is half of the window, namely 1.2 m × 0.9 m. A 3.0 m wide solar chimney is located at the left side of the room, with a cavity depth of 0.3 m and an air inlet height of 0.2 m. The dimension of cavity depth is determined by the usually obtained optimal value [18]. A cool weather condition is assumed while the ambient air is kept at 288.15 K (15 °C), and the solar radiation intensity is 500 W/m^2. The configuration of the solar chimney and room can be seen in Figs. 3–5, while the detailed inputted value can be seen in Table 4.

Comparison of the three types of solar chimney for the heating purpose can be seen in Fig. 9. Fig. 9(a) shows the volumetric flow rates along the time and the relevant hot air temperature in the chimney cavity (or the upper part of the room). It can be seen that the two solar chimney types with fresh-air heating keep at a constant airflow rate. For solar chimney under sealed heating, the airflow rate keeps decreasing along the time, while the decreasing rate keeps rising. In terms of the temperature, fresh-air heating through the room shows the highest temperature, followed by sealed heating and fresh-air heating through the cavity. The temperature rises are within a range of 13.5–21.5 K (or °C), which is quite impressive.

Fig. 9(b) presents the height of the hot layer along the time. Under a constant airflow rate through the chimney cavity, the heights of the hot layer for the two types with fresh-air heating decrease linearly with the time. For sealed heating, its decreasing rate of the hot layer height slows down along the time under the decreased airflow rate, as shown in Fig. 9(a). Solar chimney with fresh-air heating through the room takes about 401 s to achieve the steady status, while it needs about 251 s for the fresh-air heating through the cavity. The sealed heating takes the longest time, namely about 525 s, to achieve the steady status. However, the solar

Table 3
A summary of advantages and disadvantages of four solar chimney types.

Type	Schematic	Advantages	Disadvantages	Applicability
Fresh-air cooling	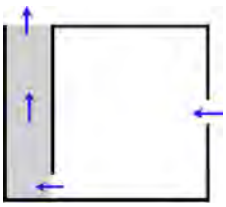	• Fresh-air exchange to keep the air quality of building; • Take away the internal heat load through the natural ventilation;	✓ Under very high-temperature weather condition, it may need to be used with other mechanical cooling.	Regularly occupied buildings under hot weather conditions
Fresh-air heating through cavity	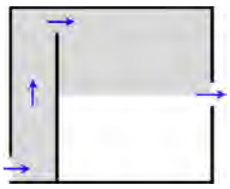	✓ Fresh-air exchange to keep the air quality of building; ✓ Averagely it shows the highest air exchange rate; ✓ The time needed to approach steady condition is relatively shorter;	• Only the upper part of room is heated, while the height is dependent on the window; • The temperature of the hot layer is relatively low;	Regularly occupied buildings under cool weather conditions
Fresh-air heating through room	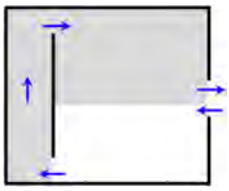	• Fresh-air exchange to keep the air quality of building; • The temperature of the hot layer is relatively higher;	✓ Only the upper part of room is heated, while the height is dependent on the window; ✓ The air exchange rate is relatively low;	Regularly occupied buildings under cold weather conditions
Sealed heating	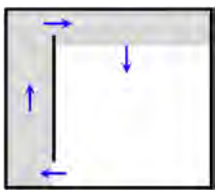	✓ Heat the whole room from ceiling to the floor;	• No fresh air supply; • The time needed to approach steady condition is relatively long;	Non-regularly occupied buildings like storages

chimney under sealed heating shows the maximum average flow rate in the first half of the room, reflected by the shortest period (about 195 s) to approach the window height.

Therefore, based on the above analysis, fresh-air heating through cavity may be the best choice under this specific cool weather condition. This is due to the following reasons: (a) the upper room shows a reasonable temperature (28.5 °C) very close to the thermal comfort temperature; (b) it shows a relatively bigger airflow rate through the chimney cavity that the room can be ventilated in a relatively short time period; and (c) most importantly, it allows fresh-air ventilation during the whole process.

5. Conclusions

Theoretical models were developed to predict solar chimney performance for four typical types under both cooling and heating

Table 4
Comparison of heating modes based on a typical room under regular cool weather conditions.

Type	Symbol	Meaning	Value	Unit
Room	A_r	Floor area of the room	36.0	m^2
	C_d	Coefficient of discharge	0.6 [48]	–
	H_c	Height of cavity/ceiling from the floor	2.7	m
	H_w	Height of window from the floor	1.35	m
	$h_{s,w}$	Height of room opening	1.2	m
	w_w	Width of room opening	0.9[a]	m
Solar chimney	d	Cavity depth	0.3	m
	$h_{s,in}$	Height (size) of air inlet	0.2	m
	w	Width of chimney cavity	3.0	m
	τ	Transmissivity of glass	0.78 [63]	–
Ambient environment	C_p	Specific heat capacity of ambient air	1005	J/kg·K
	g	Acceleration of gravity	9.8	m/s^2
	Q_{sol}	Solar radiation intensity	500	W/m^2
	T_0	Ambient temperature	288.15	K
	ρ_0	Ambient air density	1.205	kg/m^3
	μ_a	Absorption coefficient of the air	0.23 [64]	–
	δ	Stefan-Boltzmann constant	5.6704×10^{-8}	$W/m^2 \cdot K^4$

Note: [a] This is for typical sliding window with half of the area opened.

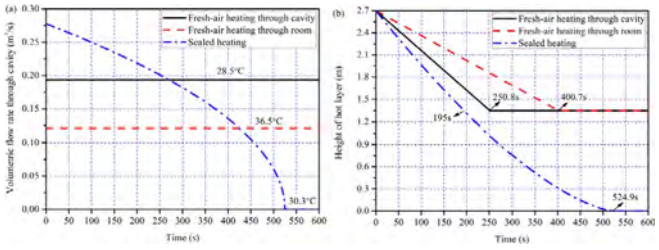

Fig. 9. A comparison of heating performance for three types of solar chimney.

modes considering room configuration, including fresh-air cooling, fresh-air heating through chimney cavity and through room, and sealed heating, as shown in Table 3. Some conclusions can be made:

- The influence of the room configuration on solar chimney performance cannot be ignored, where a roof coefficient, as shown in Eq. (55), is proposed to address the influence;
- Theoretical models were developed to predict the volumetric flow rate through the chimney cavity, which is following the same format for all the four types but with different coefficients. The models can be seen in Table 2;
- Different from cooling mode, the connected room cannot be considered as mixed ventilation with uniform temperature and air density. The whole room can be divided into two layers: the upper hot air and the lower fresh air. The volumetric flow rate of solar chimney under heating mode is not only dependent on the cavity height, but also the height of the room opening;
- Different from the other two heating modes, the volumetric flow rate through the sealed heating is dependent on the height of hot air layer. As there is no opening to exhaust those hot air, the hot air layer is approaching the floor, while the volumetric flow rate keeps decreasing with an increased descending rate; and
- To heat a typical room, fresh-air heating through cavity shows the highest volumetric flow rate and the lowest hot air temperature, which can be applied to regularly occupied buildings under cool weather conditions. Fresh-air heating through the room is in an opposite way, which is appropriate for regularly occupied buildings under cold weather conditions. For sealed heating, both the volumetric flow rate and hot air temperature are moderate, which can be applied to non-regularly occupied buildings as there is no fresh air supply.

Limitations also apply to the theoretical models developed in this study. Because of the complexity of the problem, the heat transfer inside the wall and glazing is ignored under the steady status. The interface between the hot air and ambient air in the room may go through some turbulence and external wind has influences on the solar chimney performance, which are also simplified/neglected in order to obtain the analytical solutions.

References

[1] Chen YX, Hong TZ. Impacts of building geometry modeling methods on the simulation results of urban building energy models. Appl Energy 2018;215:717–35.
[2] Kanoglu M. Renewable energy. Thermodynamics: an engineering approach. McGraw-Hill; 2015. p. 3–84.
[3] Omer AM. Energy, environment and sustainable development. Renew Sustain Energy Rev 2008;12:2265–300.
[4] Lotfabadi P. Analyzing passive solar strategies in the case of high-rise building. Renew Sustain Energy Rev 2015;52:1340–53.
[5] Burtt D, Dargusch P. The cost-effectiveness of household photovoltaic systems in reducing greenhouse gas emissions in Australia: linking subsidies with emission reductions. Appl Energy 2015;148:439–48.
[6] Shi L, Chew MYL. A review on sustainable design of renewable energy systems. Renew Sustain Energy Rev 2012;16:192–207.
[7] Khedari J, Rachapradit N, Hirunlabh J. Field study of performance of solar chimney with air-conditioned building. Energy 2003;28:1099–114.
[8] Chen YX, Hong TZ, Piette MA. Automatic generation and simulation of urban building energy models based on city datasets for city-scale building retrofit analysis. Appl Energy 2017;205:323–5.
[9] Hami K, Draoui B, Hami O. The thermal performances of a solar wall. Energy 2012;39:11–6.
[10] Amer EH. Passive options for solar cooling of buildings in arid areas. Energy 2006;31:1332–44.
[11] Perez-Lombard L, Ortiz J, Pout C. A review on buildings energy consumption information. Energy Build 2008;40:394–8.
[12] Chua KJ, Chou SK, Yang WM, Yan J. Achieving better energy-efficient air conditioning – a review of technologies and strategies. Appl Energy 2013;104:87–104.
[13] Lee KH, Strand RK. Enhancement of natural ventilation in buildings using a thermal chimney. Energy Build 2009;41:615–21.
[14] Ong KS. A mathematical model of a solar chimney. Renew Energy 2003;28:1047–60.
[15] Ong KS, Chow CC. Performance of a solar chimney. Sol Energy 2003;74:1–17.
[16] Zhai XQ, Dai YJ, Wang RZ. Experimental investigation on air heating and natural ventilation of a solar air collector. Energy Build 2005;37:373–81.
[17] Zhai XQ, Dai YJ, Wang RZ. Comparison of heating and natural ventilation in a solar house induced by two roof solar collectors. Appl Therm Eng 2005;25:741–57.
[18] Shi L, Zhang GM, Yang W, Huang DM, Cheng XD, Setunge S. Determining the influencing factors on the performance of solar chimney in buildings. Renew Sustain Energy Rev 2018;88:223–38.
[19] Li YC, Liu SL. Experimental study on thermal performance of a solar chimney combined with PCM. Appl Energy 2014;114:172–8.
[20] Amori KE, Mohanmmed SW. Experimental and numerical studies of solar chimney for natural ventilation in Iraq. Energy Build 2012;47:450–7.
[21] Burek SAM, Habeb A. Air flow and thermal efficiency characteristics in solar chimneys and Trombe Walls. Energy Build 2007;39:128–35.
[22] Lee DS, Hung TC, Lin JR, Zhao J. Experimental investigations on solar chimney for optimal heat collection to be utilized in organic Rankine cycle. Appl Energy 2015;154:651–62.
[23] Al-Kayiem HH, Sreejaya KV, Gilani SIU. Mathematical analysis of the influence of the chimney height and collector area on the performance of a roof top solar chimney. Energy Build 2014;68:305–11.
[24] Khanal R, Lei CW. Flow reversal effects on buoyancy induced air flow in a solar chimney. Sol Energy 2012;86:2783–94.
[25] Bassiouny R, Koura NSA. An analytical and numerical study of solar chimney use for room natural ventilation. Energy Build 2008;40:865–73.
[26] Spencer S. An experimental investigation of a solar chimney natural ventilation system. Canada: Concordia University; 2001.
[27] Jing HW, Chen ZD, Li AG. Experimental study of the prediction of the ventilation flow rate through solar chimney with large gap-to-height ratios. Build Environ 2015;89:150–9.
[28] Xu JL, Liu WH. Study on solar chimney used for room natural ventilation in Nanjing. Energy Build 2013;66:467–9.
[29] Shi L, Zhang GM, Cheng XD, Guo Y, Wang JH, Chew MYL. Developing an empirical model for roof solar chimney based on experimental data from various test rig. Build Environ 2016;110:115–28.
[30] Harris DJ, Helwig N. Solar chimney and building ventilation. Appl Energy 2007;84:135–46.
[31] Sakonidou EP, Karapantsios TD, Balouktsis AI, Chassapis D. Modeling of the optimum tilt of a solar chimney for maximum air flow. Sol Energy 2008;82:80–94.
[32] Nouanegue HF, Bilgen E. Heat transfer by convection, conduction and radiation in solar chimney systems for ventilation of dwellings. Int J Heat Fluid Flow 2009;30:150–7.
[33] Tan AYK, Wong NH. Natural ventilation performance of classroom with solar chimney system. Energy Build 2012;53:19–27.
[34] Letan R, Dubovsky V, Ziskind G. Enhancement of natural ventilation in high-rise residential buildings using stack system. Build Environ 2003;38:197–208.
[35] Imran AA, Jalil JM, Ahmed ST. Induced flow for ventilation and cooling by a solar chimney. Renew Energy 2015;78:236–44.
[36] Arce J, Jimenez MJ, Guaman JD, Heras MR, Alvarez G, Xaman J. Experimental study for natural ventilation on a solar chimney. Renew Energy 2009;34:2928–34.
[37] Tan AYK, Wong NH. Influences of ambient air speed and internal heat load on the performance of solar chimney in the tropics. Sol Energy 2014;102:116–25.
[38] Zamora B, Kaiser AS. Numerical study on mixed buoyancy-wind driving induced flow in a solar chimney for building ventilation. Renew Energy 2010;35:2080–8.
[39] Dimoudi A. Solar chimneys in buildings – the state of the art. Adv Build Energy Res 2009;3:21–44.
[40] Halldorsson J, Byrjalsen C, Chen ZD, Bandopadhayay P, Heiselberg P. Experimental and theoretical studies of a solar chimney with uniform heat flux. In: The 8th international conference on air distribution in rooms. Copenhagen, Denmark; 2002. p. 597–600.
[41] Andersen KT. Theory for natural ventilation by thermal buoyancy in one zone

with uniform temperature. Build Environ 2003;38:1281–9.
[42] BS 5925. Code of practice for ventilation principles and designing for natural ventilation. British Standard; 1991.
[43] Li YG. Buoyancy-driven natural ventilation in a thermally stratified one-zone building. Build Environ 2000;35:207–14.
[44] Lin YJP, Linden PF. Buoyancy-driven ventilation between two chambers. J Fluid Mech 2002;463:293–312.
[45] Andersen KT. Theoretical considerations on natural ventilation by thermal buoyancy. ASHRAE Trans 1995;15:81–93.
[46] Spencer S, Chen ZD, Li YG, Haghighat F. Experimental investigation of a solar chimney natural ventilation system. In: The 7th international conference on air distribution in rooms. Reading, U.K; 2000. p. 813–8.
[47] Afonso C, Oliveira A. Solar chimneys: simulation and experiment. Energy Build 2000;32:71–9.
[48] Linden PF. The fluid mechanics of natural ventilation. Annu Rev Fluid Mech 1999;31:201–38.
[49] Shi L, Zhang GM. An empirical model to predict the performance of typical solar chimneys considering both room and cavity configurations. Build Environ 2016;103:250–61.
[50] Zha XY, Zhang J, Qin MH. Experimental and numerical studies of solar chimney for ventilation in low energy buildings. In: Procedia Engineering - Proceedings of the 10th ISHVAC, vol. 205; 2017. p. 1612–9.
[51] Yao YZ, Cheng XD, Zhang SG, Zhu K, Zhang HP, Shi L. Maximum smoke temperature beneath the ceiling in an enclosed channel with different fire locations. Appl Therm Eng 2017;111:30–8.
[52] Zhang SG, Cheng XD, Zhu K, Yao YZ, Shi L, Zhang HP. Experimental study on curved flame characteristics under longitudinal ventilation in a subway tunnel. Appl Therm Eng 2017;114:733–43.
[53] Allocca C, Chen QY, Glicksman LR. Design analysis of single-sided natural ventilation. Energy Build 2003;35:785–95.
[54] Larsen TS, Heiselberg P. Single-sided natural ventilation driven by wind pressure and temperature difference. Energy Build 2008;40:1031–40.
[55] Dascalaki E, Santamouris M, Argiriou A, Helmis C, Asimakopoulos DN, Papadopoulos K, et al. Predicting singled sided natural ventilation rates in buildings. Sol Energy 1995;55:327–41.
[56] Gan GH. Effective depth of fresh air distribution in rooms with single-sided natural ventilation. Energy Build 2000;31:65–73.
[57] Awibi HB. Air movement in naturally-ventilated buildings. Renew Energy 1996;8:241–7.
[58] Mathur J, Bansal NK, Mathur S, Jain M, Anupma. Experimental investigations on solar chimney for room ventilation. Sol Energy 2006;80:927–35.
[59] Hui HX, Ding Y, Liu WD, Lin Y, Song YH. Operating reserve evaluation of aggregated air conditioners. Appl Energy 2017;196:218–28.
[60] Shi L, Chew MYL, Novozhilov V, Joseph P. Modelling the pyrolysis and combustion behaviours of non-charring and intumescent-protected polymers using 'FiresCone'. Polymers 2015;7:1979–97.
[61] Shi L, Chew MYL. A review of fire processes modeling of combustible materials under external heat flux. Fuel 2013;106:30–50.
[62] Bouchair A. Solar induced ventilation in the Algerian and similar climates [PhD]. UK: University of Leeds; 1989.
[63] Cengel YA, Boles MA. Thermodynamics: an engineering approach. eighth ed. McGraw-Hill; 2015.
[64] MacCracken MC. Geoengineering the climate. USA: Lawrence Livermore National Laboratory; 1991.